

## 1. Experimental section

### 1.1. Raw materials

All the raw materials including sulfur (S), lithium sulfide (Li<sub>2</sub>S), lithium bis(trifluoromethanesulfonyl)imide (LiTFSI), lithium nitrate (LiNO<sub>3</sub>), 1,3-dioxolane (DOL), 1,2-dimethoxyethane (DME), Titanium nitride (TiN), aluminum (Al) foils, polypropylene (PP) membranes (Celgard 2400), poly(vinylidene fluoride) (PVDF), N-methylpyrrolidone (NMP), lithium (Li) metal foils, carbon nanotube (CNT), graphene (G), 2032 cell shells, and 2025 cell shells were purchased from commercial sources and directly used without further purification.

### 1.2. Preparation of electrodes and electrolyte

#### 1.2.1 Preparation of G and G/TiN electrodes and characterization

100 mg G was stirred with 15 mg PVDF in NMP solvent overnight to form a homogeneous slurry with a G content of 1.5 wt.%. The G electrodes were obtained by coating the slurry on Al foils with doctor blades and dried at 60°C for 24 h. The areal loading of G was around 0.1 mg cm<sup>-2</sup>. Similarly, the G/TiN electrodes were fabricated using the same method except for introducing 100 mg TiN to form the slurry. The areal loading of TiN and G was around 0.1 mg cm<sup>-2</sup>, respectively. The G and G/TiN electrodes were cut into small disks with a diameter of 13.0 mm.

The morphologies of the G or G/TiN electrodes were observed on an FEI-Apreo C (FEI Ltd., Hillsboro state, United States) scanning electron microscope (SEM) operated at 15.00 kV. X-ray diffraction (XRD) patterns of the samples were acquired

by a Bruker D8 diffractometer with a Cu- $K_{\alpha}$  radiation in a  $2\theta$  range of  $5^{\circ}$ – $90^{\circ}$  at  $5^{\circ}$   $\text{min}^{-1}$ .

### 1.2.2 Preparation of sulfur cathodes

To prepare the sulfur cathodes without the TiN electrocatalyst, S and CNTs were first mixed in a batch with a mass ratio of 7:3 and heated at  $155^{\circ}\text{C}$  to form a composite. Then, the S/CNT composite was ball-milled with PVDF binder at a weight ratio of 9:1 in NMP to form a slurry. The as-obtained slurry was then coated on Al foils and fully dried at  $60^{\circ}\text{C}$  for 24 h. Similarly, the sulfur cathodes with the TiN electrocatalyst were prepared using the same method except for introducing the TiN electrocatalyst. The mass ratio of the TiN electrocatalyst to S was 1:7. The areal sulfur loading of the two cathodes was controlled at  $5.0 \text{ mg}_S \text{ cm}^{-2}$  to make a fair comparison. The sulfur cathodes with or without the TiN electrocatalyst were cut into small disks with a diameter of 15.0 mm.

### 1.2.3 Preparation of electrolyte

For the electrolyte of Li–S coin cells, the blank electrolyte was mixed solvents of DOL/DME (v/v = 1:1) with  $1.0 \text{ mol L}^{-1}$  LiTFSI and 2.0 wt.%  $\text{LiNO}_3$ .

In order to prepare the  $\text{Li}_2\text{S}_6$  electrolyte, S and  $\text{Li}_2\text{S}$  powders were weighed at a stoichiometric molar ratio of 5:1 and then mixed in DOL/DME (1:1, by vol.) solvents with  $1.0 \text{ mol L}^{-1}$  LiTFSI. The mixture was stirred at  $50^{\circ}\text{C}$  to prepare the  $\text{Li}_2\text{S}_6$  electrolyte with a sulfur concentration of 0.20, 1.0, or  $2.0 \text{ mol}_{[\text{S}]} \text{ L}^{-1}$ .  $\text{Li}_2\text{S}_8$  electrolyte

was prepared by using the similar method. S and Li<sub>2</sub>S powders were weighed at a stoichiometric molar ratio of 7:1 and then mixed in DOL/DME (1:1, by vol.) solvents with 1.0 mol L<sup>-1</sup> LiTFSI and 2.0 wt.% LiNO<sub>3</sub>. The mixture was stirred at 50°C to prepare the Li<sub>2</sub>S<sub>8</sub> electrolyte with a sulfur concentration of 0.20, 1.0, or 2.0 mol<sub>[S]</sub> L<sup>-1</sup>. All the above procedures were conducted in an Ar-filled glove box with water and oxygen contents below 0.1 ppm.

### *1.3. Kinetics evaluation*

#### *1.3.1. Liquid–liquid conversion kinetics*

Li<sub>2</sub>S<sub>6</sub> symmetric cells were assembled to evaluate the liquid–liquid conversion kinetics. G or G/TiN electrodes were used as the current collectors in Li<sub>2</sub>S<sub>6</sub> symmetric cells. Concretely, two G electrodes were assembled into a standard 2025 coin cell with a PP separator (19.0 mm in diameter). 20 μL Li<sub>2</sub>S<sub>6</sub> electrolyte with the sulfur concentration of 0.20, 1.0, or 2.0 mol<sub>[S]</sub> L<sup>-1</sup> were added to each side of the electrodes to assemble the Li<sub>2</sub>S<sub>6</sub> symmetrical cells. Electrochemical impedance spectroscopy (EIS) and cyclic voltammetry (CV) curves were collected on a Solartron 1470E electrochemical workstation. EIS was conducted at the open circuit voltage with a sinusoidal voltage amplitude of 10 mV and a frequency spectrum ranging from 0.1 Hz to 10 kHz. CV measurements were conducted between -0.4 and 0.4 V at a scan rate of 50 mV s<sup>-1</sup>. The maximum current of the CV curves ( $I_{\max}$ ) and the charge transfer resistance ( $R_{\text{ct}}$ ) of the EIS curve are selected to evaluate the liquid–liquid conversion kinetics.

### 1.3.2. Liquid–solid conversion kinetics

Li | Li<sub>2</sub>S<sub>8</sub> cells with the sulfur concentration of 0.20, 1.0, or 2.0 mol<sub>[S]</sub> L<sup>-1</sup> were assembled to study the liquid–solid conversion kinetics. The G or G/TiN electrode was used as the cathodic current collector and a 600 μm Li metal foil with a diameter of 16.0 mm was used as the anode. PP membranes with a diameter of 19.0 mm were used as the separator. The catholyte was 20 μL Li<sub>2</sub>S<sub>8</sub> electrolyte with a sulfur concentration of 0.20, 1.0, or 2.0 mol<sub>[S]</sub> L<sup>-1</sup>, and the anolyte was 5 μL blank electrolyte. Potentiostatic intermittent titration technique (PITT) tests were performed on the Li | Li<sub>2</sub>S<sub>8</sub> cells. The Li | Li<sub>2</sub>S<sub>8</sub> cells were potentiostatically discharged at 2.30, 2.25, 2.20, 2.18, and 2.16 V for 2.0 h and then potentiostatically discharged at 2.15, 2.14, 2.13, and 2.12 V for 8.0 h and finally potentiostatically discharged at 2.05 V for 30.0 h. The peak current ( $I_{\text{peak}}$ ) and Li<sub>2</sub>S deposition capacity ( $Q$ ) were collected to evaluate the nucleation and growth behaviors of Li<sub>2</sub>S. Notably, the Li<sub>2</sub>S deposition capacity was obtained by integrating the current curve and time at 2.05 V.

### 1.3.3 Comparison of the kinetics parameters

The kinetics promotion effectiveness of the TiN electrocatalyst on the liquid–liquid and liquid–solid conversion kinetics at different sulfur concentrations were calculated based on the following equation (taking  $I_{\text{peak}}$  as an example):

$$\text{Promotion(\%)} = \left| \frac{I_{\text{peak (W)}} - I_{\text{peak (O)}}}{I_{\text{peak (O)}}} \right| \times 100\%$$

where the  $I_{\text{peak (O)}}$  is the peak current of the Li | Li<sub>2</sub>S<sub>8</sub> cells without the TiN electrocatalyst, and the  $I_{\text{peak (W)}}$  is the peak current of Li | Li<sub>2</sub>S<sub>8</sub> cells with the TiN electrocatalyst. Notably, the kinetics promotion effectiveness of the TiN electrocatalyst on  $I_{\text{max}}$  increase,  $R_{\text{ct}}$  decrease, and  $Q$  increase were calculated in the same way.

#### *1.3.4 Shuttle effect suppression*

Li | Li<sub>2</sub>S<sub>8</sub> cells were assembled following the procedure in section 1.3.2. to evaluate the shuttle current. The catholyte was 20  $\mu\text{L}$  Li<sub>2</sub>S<sub>8</sub> electrolyte without LiNO<sub>3</sub> addition with the sulfur concentration of 0.20, 1.0, or 2.0 mol<sub>[S]</sub> L<sup>-1</sup>, and the anolyte was 5  $\mu\text{L}$  blank electrolyte without LiNO<sub>3</sub> as well. The Li | Li<sub>2</sub>S<sub>8</sub> cells were discharged to 2.15 V at current of 0.5 mA and then potentiostatically charged at 2.30, 2.32, 2.34, 2.36, and 2.38 V for 10.0 h. The stable charging currents at 10.0 h were collected as the shuttle current to quantitatively evaluate the shuttle effect of lithium polysulfides.

### *1.4. Li-S coin cells assembly and electrochemical measurements*

#### *1.4.1 Li-S coin cells assembly*

Li-S coin cells with or without the TiN electrocatalyst were assembled with standard 2032 coin-type cells under different E/S ratio conditions. Concretely, the 5.0 mg<sub>S</sub> cm<sup>-2</sup> sulfur cathodes with a diameter of 15.0 mm were used as the cathode, 600  $\mu\text{m}$  lithium metal foils with a diameter of 16.0 mm were adopted as the anode, and PP membranes with a diameter of 19.0 mm were used as the separator. Concretely, 48, 35, 30, or 26  $\mu\text{L}$  of the blank electrolyte was added to the cathode side and 5  $\mu\text{L}$  of the blank electrolyte was added to the anode side to wet the surface of the anode for the cells with

the E/S ratio of 6.0, 4.5, 4.0, or 3.5  $\mu\text{L mg}^{-1}$ , respectively. All the above procedures were conducted in an argon-filled glove box with water and oxygen contents below 0.1 ppm.

#### *1.4.2 Performance evaluation of the Li–S coin cells*

Li–S coin cells with or without the TiN electrocatalyst were galvanostatically cycled between 1.70–2.60 V on a Neware multichannel battery cycler under different C-rates (1 C = 1672 mA g<sup>-1</sup>). To evaluate the rate performances, the cells were activated at 0.05 C for 2 cycles and then cycled at 0.1 C and 0.15 C for 3 cycles at each rate.

The polarization and discharge capacity of the Li–S coin cells were used to quantitatively evaluate the kinetics promotion effectiveness of the TiN electrocatalyst. The polarization was obtained by the difference between the thermodynamic medium voltage and the kinetic medium voltage. The medium voltage is the voltage at half the discharge capacity. The thermodynamic medium voltage is obtained through galvanostatic intermittent titration technique (GITT). GITT tests of the Li–S coin cells were conducted following the procedure provided in Section 1.5. According to the results, the thermodynamic medium voltage of the second discharge plateau keeps at 2.163 V on average despite under different working conditions (**Figure S19, S21, and S23**). Therefore, the thermodynamic medium voltage is regarded as 2.163 V for comparison. The kinetic medium voltage is obtained through the discharge curves at each respective rate. Then, the discharge capacity increase and polarization decrease with the help of the TiN electrocatalyst at each E/S ratio condition were quantitatively

calculated to evaluate the kinetics promotion effectiveness of the TiN electrocatalyst.

### 1.5. Polarization decoupling of lean-electrolyte Li–S batteries

An EIS combined GITT (EIS–GITT) method was used to decouple the polarization of Li–S cells without the TiN electrocatalyst at the E/S ratio = 6.0 or 4.0  $\mu\text{L mg}^{-1}$  and with the TiN electrocatalyst at the E/S ratio = 4.0  $\mu\text{L mg}^{-1}$ . The Li–S cells were assembled following the same procedure as section 1.4.1. The GITT curves were obtained by a series of galvanostatic discharge processes of 4.0 min at 0.15 C followed by 60.0 min rest at each step. An additional EIS measurement was conducted before the galvanostatic discharge process to obtain the ohmic resistance ( $R_{\text{ohm}}$ ). EIS was conducted at the open circuit voltage with a sinusoidal voltage amplitude of 10 mV and a frequency spectrum ranging from 0.1 Hz to 10 kHz. The ohmic resistance was obtained by the intercept at the  $Z'$  axis.

$\eta_{\text{total}}$  was determined as the voltage difference between the thermodynamic voltage and the kinetic voltage of the Li–S cells and can be divided into concentration ( $\eta_{\text{con}}$ ), ohmic ( $\eta_{\text{ohm}}$ ), and activation polarization ( $\eta_{\text{ac}}$ ). The voltage recovery during the rest step in GITT was resulted from the concentration gradient built in the discharge step and was adopted as the  $\eta_{\text{con}}$ .  $\eta_{\text{ohm}}$  was determined by multiplying the ohmic resistance obtained through the EIS measurements with the applied current density.  $\eta_{\text{ac}}$  was obtained through  $\eta_{\text{ac}} = \eta_{\text{total}} - \eta_{\text{ohm}} - \eta_{\text{con}}$ .

## *1.6. Assembly and electrochemical test of Li–S pouch cells*

### *1.6.1 Fabrication of sulfur cathodes with or without the TiN electrocatalyst and lithium anodes*

To prepare the sulfur cathodes without the TiN electrocatalyst, S and MWCNTs were first mixed in a batch with a mass ratio of 7:1 and heated at 155°C to form a composite. The composite was then ball-milled with PVDF binder at a weight ratio of 9:1 in NMP to form a homogeneous slurry. The as-obtained slurry was then coated on both sides of Al foils. The sulfur cathodes were cut into 4.0 cm × 7.0 cm electrodes after being fully dried at 60°C for 24.0 h. Similarly, the TiN electrocatalyst with a mass ratio to S of 0.5:7 was added to the slurry, and sulfur cathodes with the TiN electrocatalyst were prepared following the same procedure. The areal sulfur loading of both the sulfur cathodes was  $7.5 \pm 0.2 \text{ mg}_S \text{ cm}^{-2}$  on a single side. Lithium anodes were fabricated by rolling lithium metal foils on both sides of Cu foils and then cut into electrodes of the same size as the sulfur cathodes. The thickness of the lithium foil was 75 μm on a single side.

### *1.6.2. Assembly and test of Li–S pouch cells*

The separator used in pouch cells was Celgard 2400 PP membranes. The basic electrolyte was 1.0 mol L<sup>-1</sup> LiTFSI dissolved in a mixed solvent of DOL and DME (v/v=1/1) with 5 wt% LiNO<sub>3</sub> additives.

To assemble Li–S pouch cells at 2 Ah level, three double-side sulfur cathodes and four double-side lithium anodes were stacked layer-by-layer separated by the PP



membranes. All the electrodes were set in parallel connection and then put in a package. Then, the basic electrolyte was injected into the pouch cell and the E/S ratio was  $3.0 \text{ g}_{\text{ele}} \text{ mgs}^{-1}$ . After that, the pouch cell was vacuumed ( $-65 \text{ kPa}$ ) and sealed for further electrochemical tests.

The as-assembled Li-S pouch cells were rested for 12.0 h firstly and then galvanostatically cycled between 1.70–2.55 V on a Land multichannel battery tester (Wuhan Land Electronic Co., Ltd.) at the current density of 0.05 C (1 C =  $1000 \text{ mA g}_s^{-1}$ ). The energy density of the Li-S pouch cell was calculated based on all cell components including cathode, separator, anode, electrolyte, current collector, tabs, and cell package.

## 2. Supplementary figures

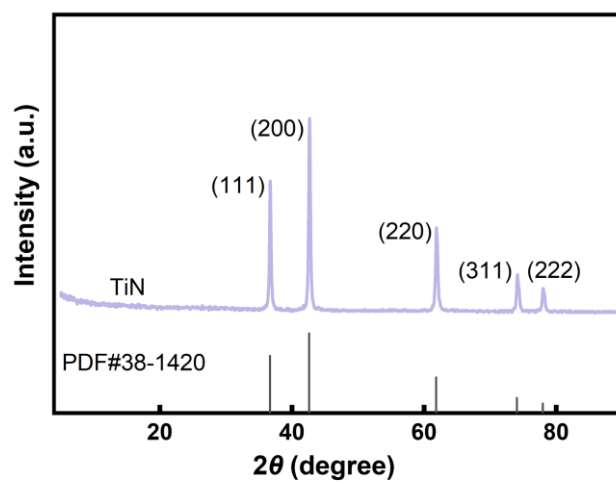


**Figure S1.** XRD patterns of the TiN electrocatalyst.

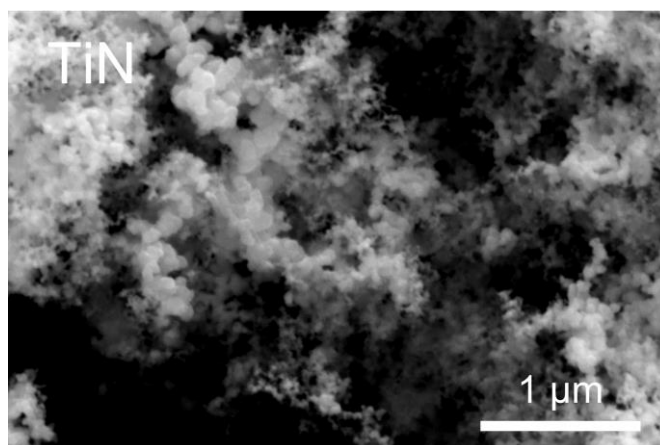


**Figure S2.** SEM image of the TiN electrocatalyst.

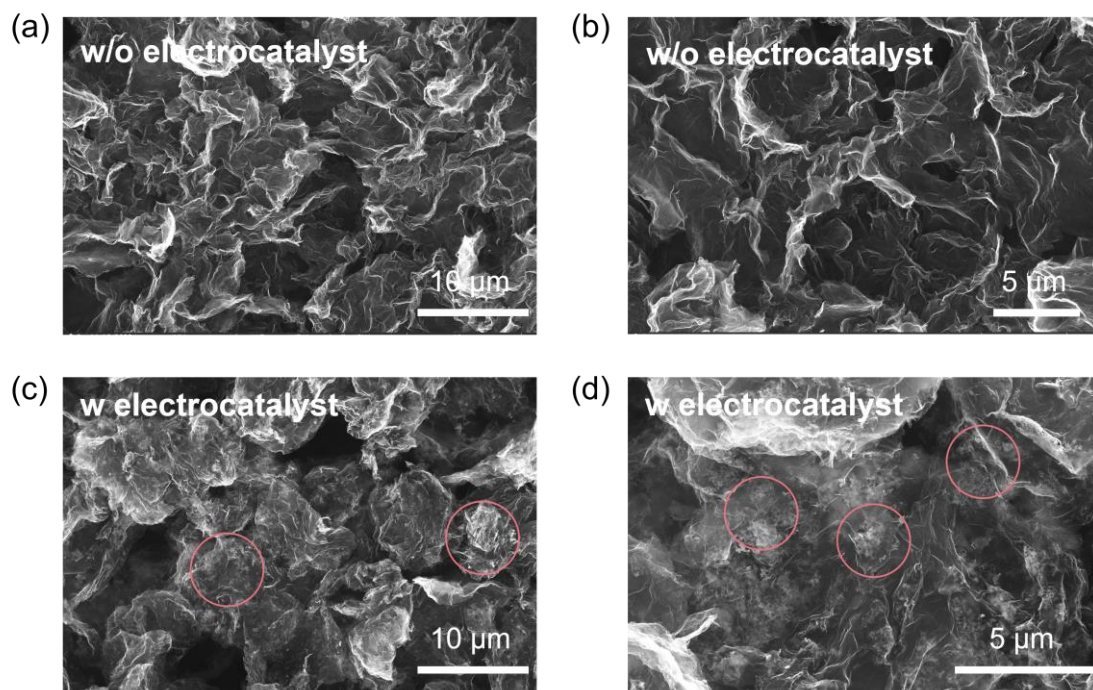


**Figure S3.** SEM images of (a, b) the G electrode and (c, d) the G/TiN electrode.

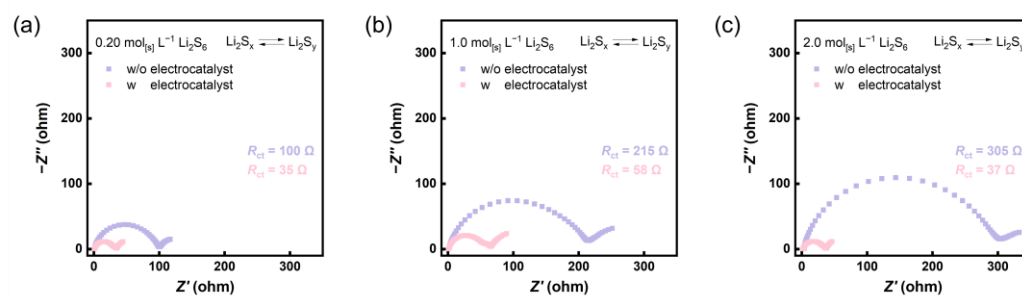


**Figure S4.** Nyquist plots of the  $\text{Li}_2\text{S}_6$  symmetric cells with (red) and without (purple) the TiN electrocatalyst at the sulfur concentration of (a)  $0.20 \text{ mol}_{[\text{S}]} \text{ L}^{-1}$ , (b)  $1.0 \text{ mol}_{[\text{S}]} \text{ L}^{-1}$ , and (c)  $2.0 \text{ mol}_{[\text{S}]} \text{ L}^{-1}$ .

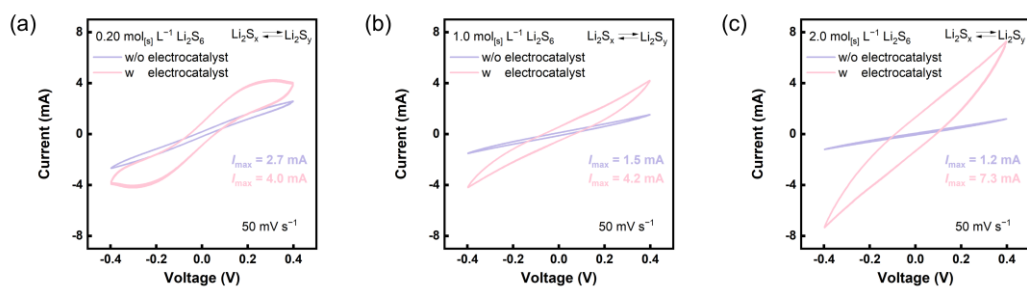


**Figure S5.** CV curves of the  $\text{Li}_2\text{S}_6$  symmetric cells with (red) and without (purple) the TiN electrocatalyst at the sulfur concentration of (a)  $0.20 \text{ mol}_{[\text{S}]} \text{ L}^{-1}$ , (b)  $1.0 \text{ mol}_{[\text{S}]} \text{ L}^{-1}$ , and (c)  $2.0 \text{ mol}_{[\text{S}]} \text{ L}^{-1}$ .

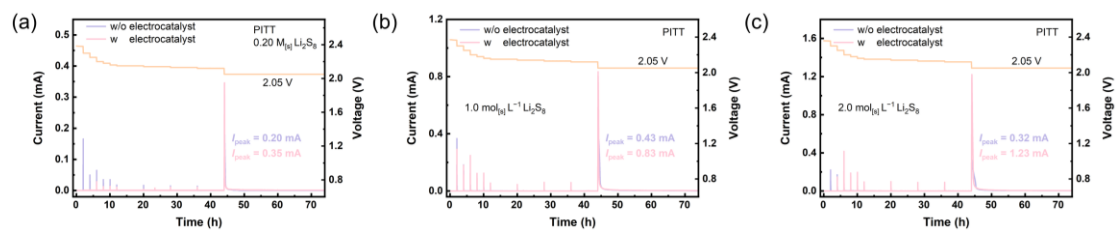


**Figure S6.** PITT curves of the Li | Li<sub>2</sub>S<sub>8</sub> cells with (red) and without (purple) the TiN electrocatalyst at the sulfur concentration of (a) 0.20 mol<sub>[S]</sub> L<sup>-1</sup>, (b) 1.0 mol<sub>[S]</sub> L<sup>-1</sup>, and (c) 2.0 mol<sub>[S]</sub> L<sup>-1</sup>.

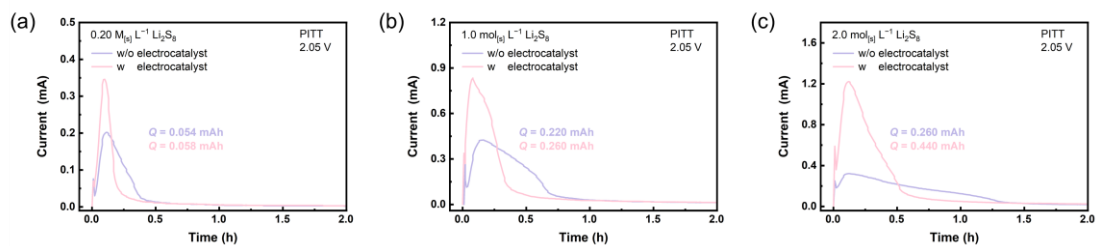


**Figure S7.** Current–time curves of the Li | Li<sub>2</sub>S<sub>8</sub> cells with (red) and without (purple) the TiN electrocatalyst at the voltage of 2.05 V with the sulfur concentration of (a) 0.20 mol<sub>[S]</sub> L<sup>-1</sup>, (b) 1.0 mol<sub>[S]</sub> L<sup>-1</sup>, and (c) 2.0 mol<sub>[S]</sub> L<sup>-1</sup>.



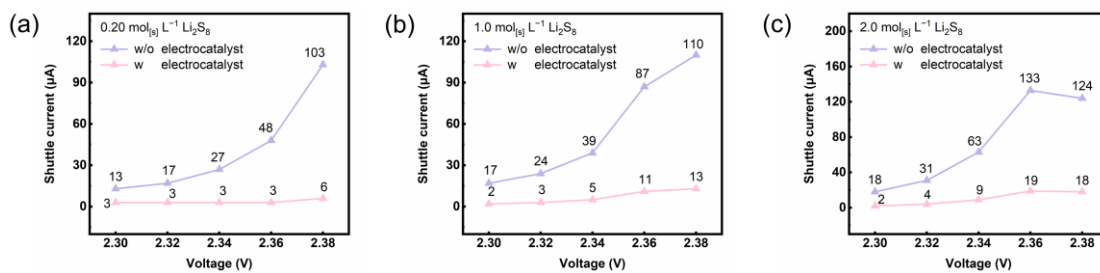


**Figure S8.** Shuttle current of  $\text{Li} | \text{Li}_2\text{S}_8$  cells with (red) or without (purple) the TiN electrocatalyst at the sulfur concentration of (a)  $0.20 \text{ mol}_{[\text{S}]} \text{ L}^{-1}$ , (b)  $1.0 \text{ mol}_{[\text{S}]} \text{ L}^{-1}$ , and (c)  $2.0 \text{ mol}_{[\text{S}]} \text{ L}^{-1}$ .

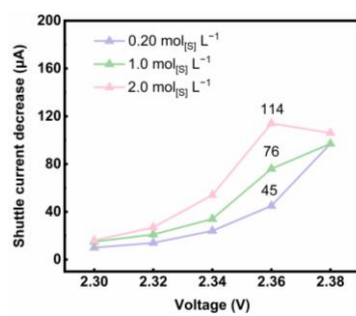


**Figure S9.** Shuttle current decreases of Li | Li<sub>2</sub>S<sub>8</sub> cells at the sulfur concentration of 0.20, 1.0, or 2.0 mol<sub>[S]</sub> L<sup>-1</sup> using the TiN electrocatalyst.

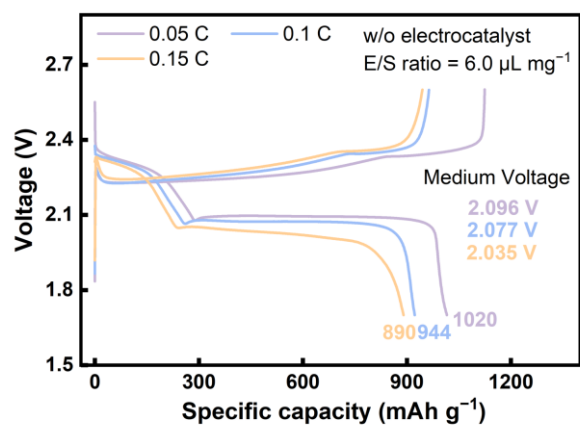


**Figure S10.** Charge–discharge profiles of the Li–S coin cells without the TiN electrocatalyst at 0.05, 0.1, and 0.15 C at the E/S ratio = 6.0  $\mu\text{L mg}^{-1}$ .

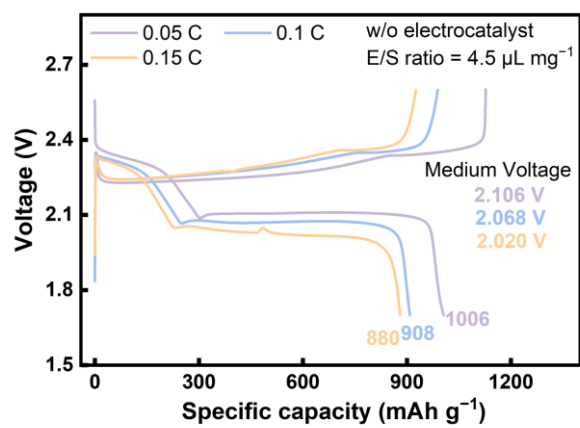


**Figure S11.** Charge–discharge profiles of the Li–S coin cells without the TiN electrocatalyst at 0.05, 0.1, and 0.15 C at the E/S ratio = 4.5 μL mg<sup>-1</sup>.

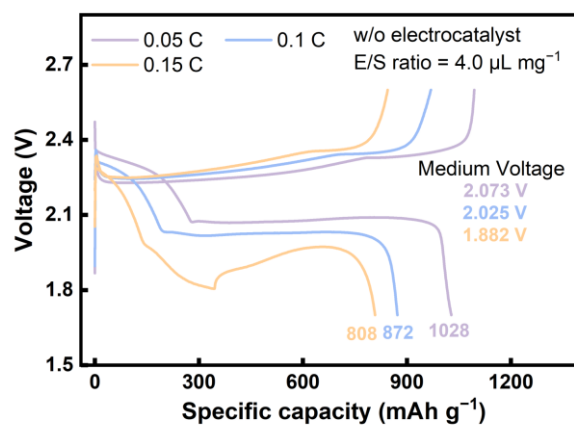


**Figure S12.** Charge–discharge profiles of the Li–S coin cells without the TiN electrocatalyst at 0.05, 0.1, and 0.15 C at the E/S ratio = 4.0 μL mg<sup>-1</sup>.

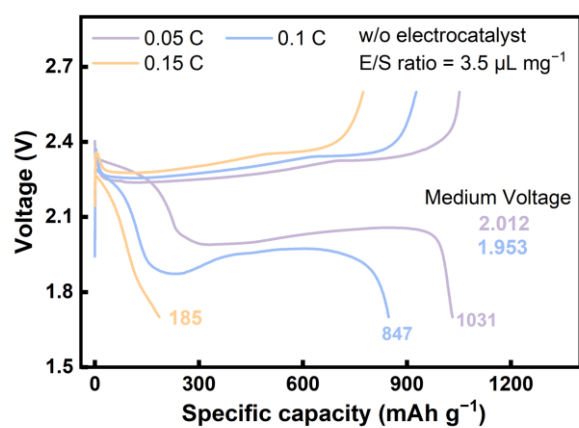


**Figure S13.** Charge–discharge profiles of the Li–S coin cells without the TiN electrocatalyst at 0.05, 0.1, and 0.15 C at the E/S ratio = 3.5 μL mg<sup>-1</sup>.

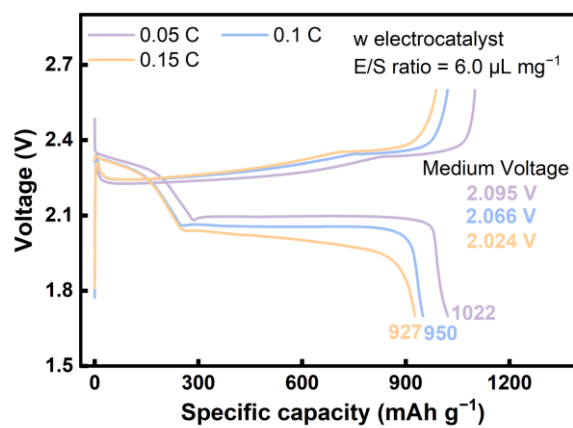


**Figure S14.** Charge–discharge profiles of the Li–S coin cells with the TiN electrocatalyst at 0.05, 0.1, and 0.15 C at the E/S ratio = 6.0  $\mu\text{L mg}^{-1}$ .

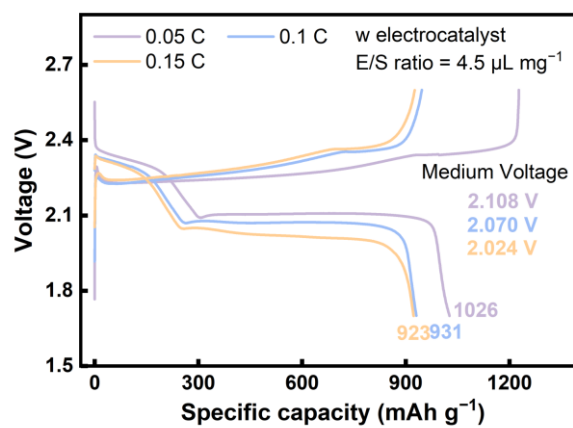


**Figure S15.** Charge–discharge profiles profiles of the Li–S coin cells with the TiN electrocatalyst at 0.05, 0.1, and 0.15 C at the E/S ratio = 4.5 μL mg<sup>-1</sup>.



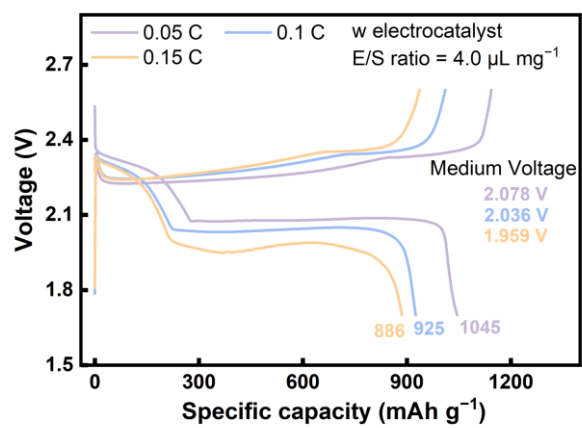


**Figure S16.** Charge–discharge profiles of the Li–S coin cells with the TiN electrocatalyst at 0.05, 0.1, and 0.15 C at the E/S ratio = 4.0  $\mu\text{L mg}^{-1}$ .

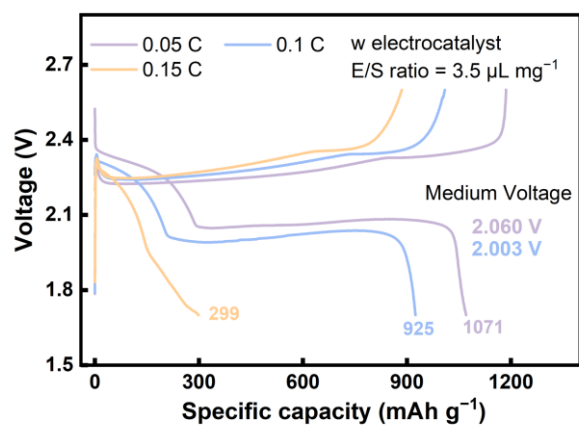


**Figure S17.** Charge–discharge profiles of the Li–S coin cells with the TiN electrocatalyst at 0.05, 0.1, and 0.15 C at the E/S ratio = 3.5 μL mg<sup>-1</sup>.

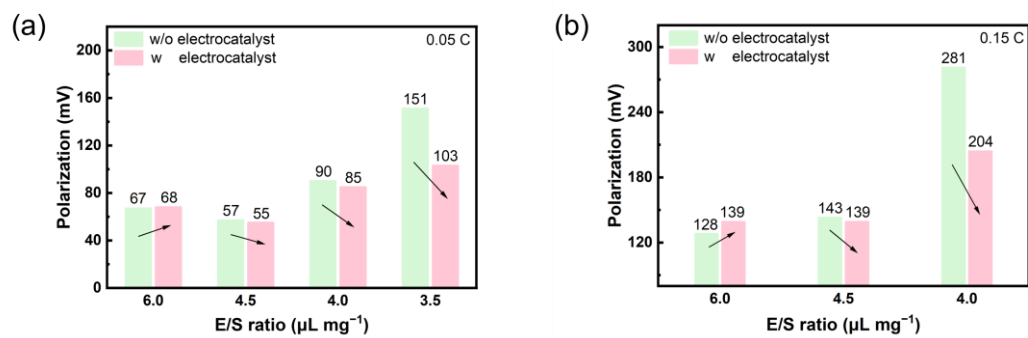


**Figure S18.** Polarization of Li-S coin cells with (red) and without (green) the TiN electrocatalyst at the E/S ratios of 6.0, 4.5, 4.0, or 3.5  $\mu\text{L mg}^{-1}$  at the discharge rates of (a) 0.05 C and (b) 0.15 C.

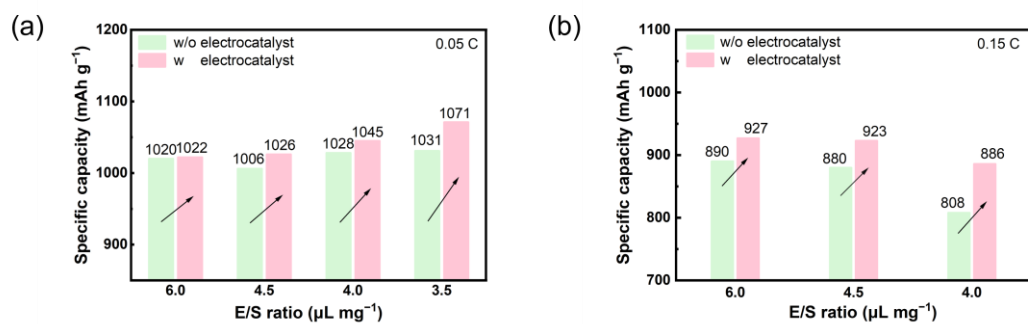


**Figure S19.** Discharge capacity of Li-S coin cells with (red) and without the TiN electrocatalyst (green) at the E/S ratios of 6.0, 4.5, 4.0, or 3.5 μL mg<sup>-1</sup> at the discharge rates of (a) 0.05 C and (b) 0.15 C.

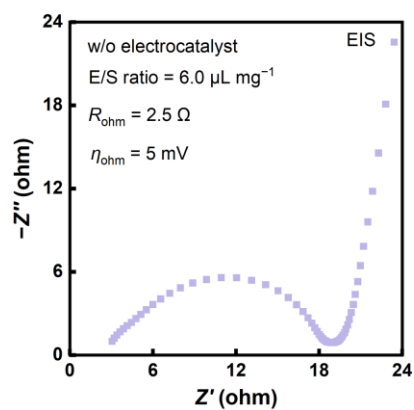


**Figure S20.** Nyquist plot of the Li-S coin cell without the TiN electrocatalyst at the E/S ratio =  $6.0 \mu\text{L mg}^{-1}$ .

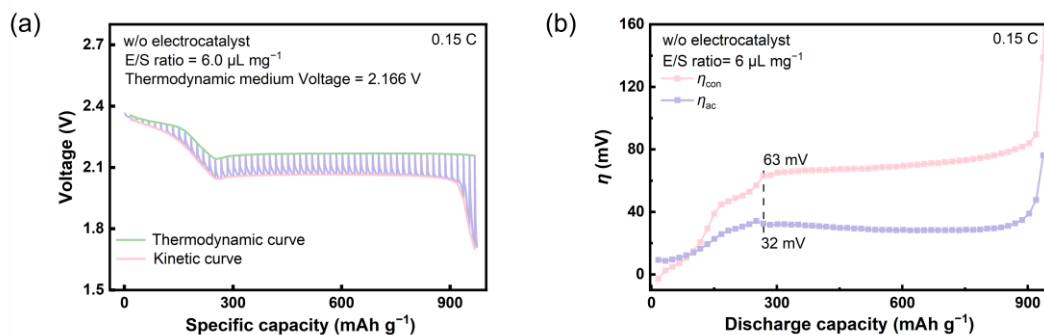


**Figure S21.** (a) Discharge GITT curves of the Li-S coin cell without the TiN electrocatalyst at the E/S ratio of  $6.0 \mu\text{L mg}^{-1}$  at  $0.15 \text{ C}$ . Notably, the red curve is kinetic voltage curve and the green curve is thermodynamic voltage curve. (b)  $\eta_{\text{con}}$  (red) and  $\eta_{\text{ac}}$  (purple) of the Li-S coin cell without the TiN electrocatalyst during the discharge process at the E/S ratio of  $6.0 \mu\text{L mg}^{-1}$  at  $0.15 \text{ C}$ .

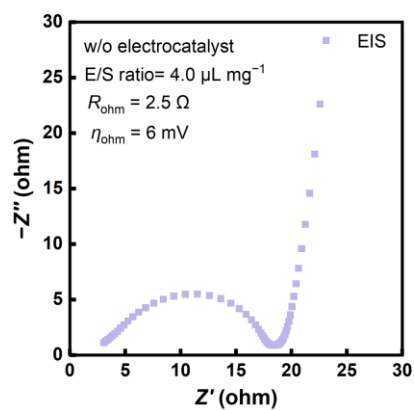


**Figure S22.** Nyquist plot of the Li-S coin cell without the TiN electrocatalyst at the E/S ratio = 4.0  $\mu\text{L mg}^{-1}$ .

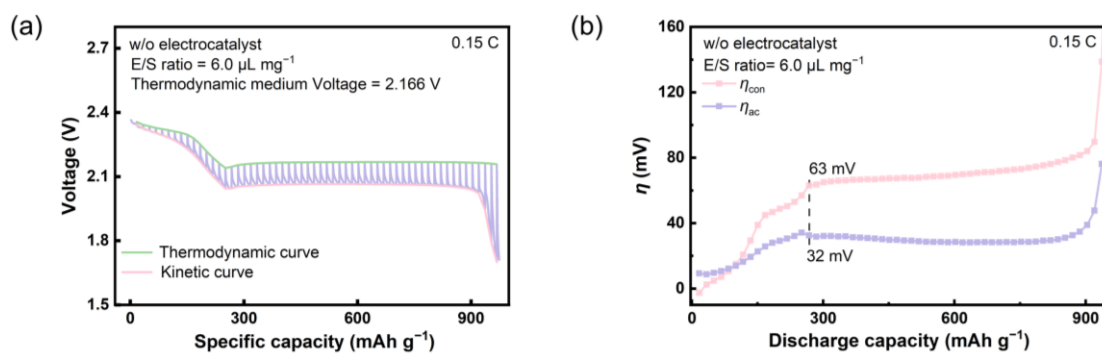


**Figure S23.** (a) Discharge GITT curves of the Li-S coin cell without the TiN electrocatalyst at the E/S ratio of  $4.0 \mu\text{L mg}^{-1}$  at  $0.15 \text{ C}$ . Notably, the red curve is kinetic voltage curve and the green curve is thermodynamic voltage curve. (b)  $\eta_{\text{con}}$  (red) and  $\eta_{\text{ac}}$  (purple) of the Li-S coin cell without the TiN electrocatalyst during the discharge process at the E/S ratio of  $4.0 \mu\text{L mg}^{-1}$  at  $0.15 \text{ C}$ .



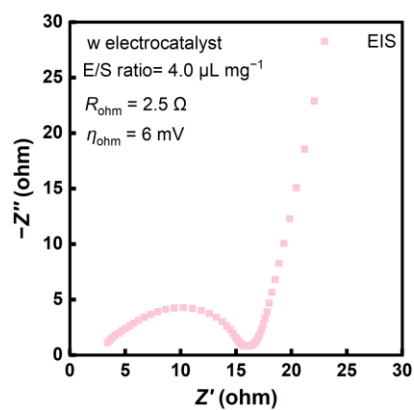


**Figure S24.** Nyquist plot of the Li-S coin cell with the TiN electrocatalyst at the E/S ratio = 4.0  $\mu\text{L mg}^{-1}$ .

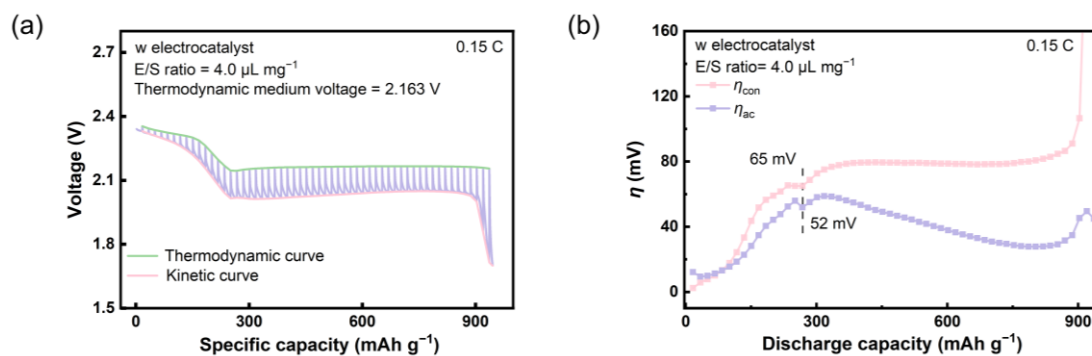


**Figure S25.** (a) Discharge GITT curves of the Li-S coin cell with the TiN electrocatalyst at the E/S ratio of  $4.0 \mu\text{L mg}^{-1}$  at  $0.15 \text{ C}$ . Notably, the red curve is kinetic voltage curve and the green curve is thermodynamic voltage curve. (b)  $\eta_{\text{con}}$  (red) and  $\eta_{\text{ac}}$  (purple) of the Li-S coin cell with the TiN electrocatalyst during the discharge process at the E/S ratio of  $4.0 \mu\text{L mg}^{-1}$  at  $0.15 \text{ C}$ .

### 3. Supplementary table

**Table S1.** Components and energy density of the Li–S pouch cells with or without the TiN electrocatalyst.

Items	Pouch cell without TiN	Pouch cell with TiN
Electrode piles (g)	3.79	3.84
Electrolyte mass (g)	3.82	3.73
Cell package (g)	2.10	2.10
Total mass (g)	9.71	9.67
Energy (Wh)	2.58	3.07
Energy density (Wh kg <sup>-1</sup> )	266	317